IEEE Access
Multidisciplinary | Rapid Review | Open Access Journal

Received July 9, 2016, accepted July 22, 2016, date of publication August 3, 2016, date of current version September 16, 2016.

Digital Object Identifier 10.1109/ACCESS.2016.2597869

Evolutionary Design of Adjustable Six-Linkage Bar Manufacturing Mechanisms Using Niche Genetic Algorithms

CHIU-HUNG CHEN[1] and JYH-HORNG CHOU[2,3,4], (Fellow, IEEE)

[1]Department of Information Technology, Kao Yuan University, Kaohsiung 82151, Taiwan
[2]Institute of Engineering Science and Technology, National Kaohsiung First University of Science and Technology, Kaohsiung 824, Taiwan
[3]Department of Electrical Engineering, National Kaohsiung University of Applied Sciences, Kaohsiung 807, Taiwan
[4]Department of Healthcare Administration and Medical Informatics, Kaohsiung Medical University, Kaohsiung 807, Taiwan

Corresponding author: J.-H. Chou (choujh@kuas.edu.tw)

This paper was supported by the Ministry of Science and Technology, Taiwan, under Grant MOST105-2218-E-151-001, Grant MOST 103-2221-E-244-019, and Grant MOST 104-2221-E-244-017.

ABSTRACT This paper studies the optimal synthesis design of adjustable six-linkage mechanisms in metal-mold die-casting systems. The synthesis process is extremely complex because of higher order structures, collision-free constraints, and multiple loci in the solution space. Therefore, a twin-space crowding genetic algorithm was used to solve the design problem with the multiplicity of solutions. To verify the effectiveness of the proposed approach, this paper first studied the function generation problems for adjustable four linkage-bar structures in the literature, and compared these with a numerical local optimization method. From the comparison result, multiple and more precise design solutions can be obtained with the proposed approach. The synthesis design problem for collision-free adjustable six-linkage bars was then solved and discussed. The simulated experiments demonstrated the promising result of the proposed approach.

INDEX TERMS Adjustable mechanism, evolutionary algorithm, collision-free design.

I. INTRODUCTION

Industry companies typically adopt linkage mechanisms to perform dedicated manufacturing tasks because of their cost-efficient, fast and stable operations compared to other types of devices such as serial-link robots. However, because of the limited degrees of freedom for planar linkages, it is difficult to synthesize linkage structures to satisfy complex tasks, such as performing an exact function generation and supporting multiple manufacturing paths [1]–[3]. Adjustable linkages are often used in these situations.

Some studies have explored the synthesis design of adjustable linkages based on an adjustable pivot position [4]. These studies mainly focused on motion generation [5] or function generation [6]. Naik and Amarnath [7] designed a five-bar linkage and used the fifth bar to adjust the pivot for motion generation problems. Zhou [8] used a similar design for function generation tasks, but added additional three bars to cooperate with the fifth bar to form a parallel four-edged shape. Ganesan and Sekar [9] designed a four-linkage-bar with an adjustable ground pivot to generate a rectangular path.

Other studies have designed linkage-bars with adjustable bar lengths to solve the synthesis problem. Hong and Erdman [10] studied planar and spatial adjustable four-linkage bar structures with adjustable input and output bar lengths to perform motion guiders. Soong and Chang [11] studied a procedure to solve function-generation problems for four-bar linkages with variable length driving links. However, it is difficult to synthesize stricter paths for low-order linkage structures, and as such a higher-order structure is chosen. For example, Shimojima et al. [12] designed six-linkage bars with twin four-linkage-bar structures based on a shared symmetrical bar to generate a straight line and an L-shaped path.

This paper studies the design problem of a transfer mechanism used in a metal-mold die-casting system (Fig. 1). The mechanism performs a flexible transfer task containing multiple operation modes. In the operation flow, it loads different types of metal liquids, such as aluminum alloy and magnesium aluminum alloy, in different modes and transfers them to different injection holes to ensure a favorable manufacturing quality. Because of the difficulty in synthesizing multiple

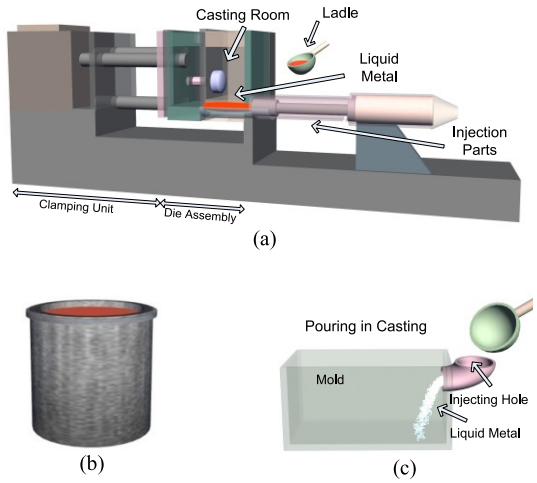

FIGURE 1. Metal-mold die-casting system. (a) Metal-mold die-casting machine (from http://www.custompartnet.com/). (b) Boiler (loading area). (c) Injection Position.

manufacturing paths, an adjustable six-linkage-bar structure was considered.

When synthesizing such high-order and adjustable linkage structures, if the designed structures are insufficiently precise, the accumulated component errors will result in high failure rates and the structures will be unsuitable for practical manufacturing work. Therefore, many studies [13], [14] have investigated various synthesis techniques for the kinematical analysis of linkages. Graphical and analytical methods are the most explored techniques in the literature [15] but their applications are limited to finite precision points [16]. As computing power has grown, optimization methods have been used to improve solution capabilities. By minimizing coupling errors in the objective function, some evolutionary methods have been developed to solve optimal design problems [17]–[19]. However, the evolutionary synthesis of adjustable linkages for multiple manufacturing paths has rarely been discussed in literature. In this paper, we study an evolutionary approach to solve the precise synthesis of adjustable linkages on the basis of kinematical analysis including position, velocity and acceleration under a collision-free constraint. Moreover, to assist the design work, this paper further studied the solution multiplicity of synthesis design problems. In practice, it is of great help to mechanism designers to have multiple design solutions for choice.

In literature, genetic algorithms (GAs) have been proved to be able to achieve optimization through mimicking processes observed in natural evolution [20]–[22]. However, a simple GA (SGA) [23] cannot efficiently maintain multiple local or global solutions. Therefore, our previous work [24] has studied a niche genetic algorithm, the twin-space crowding GA (TSCGA), which improved the diversity of the SGA to efficiently explore multiple global solutions. Furthermore, its parameter-free paradigm is more suitable for engineering problems compared to other niche mechanisms with specific parameters such as the niche radius [25], [26]. Therefore, this paper used the TSCGA to solve the design problems.

To verify the solution capability of the proposed approach, this study first examines the optimal function generation problems of adjustable four-bar linkages and compares the synthesis result with the previous work of Zhou [8]. The collision-free design problem of the adjustable six-bar ladle is then studied. In the ladle design, the proposed approach explored multiple design solutions which simultaneously satisfy the dimension synthesis, multiple paths and practical manufacturing constraints such as kinematical acceleration and collision-free constraints. These diverse solutions were studied and discussed in the simulated experiments.

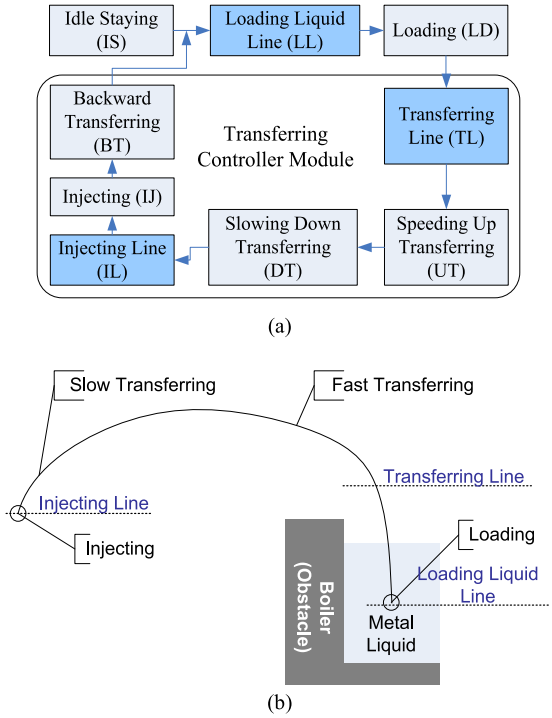

FIGURE 2. Transfer operation diagram. (a) Controller module block. (b) Transferring curve.

II. PROBLEM DEFINITION AND FORMULATION

The operation principle of the ladle mechanism is shown in Fig. 2. In each transfer cycle, it first stops at the loading liquid line, and then begins to load the metal liquid. During the process, the ladle should reach the loading area without colliding with the boiler shell and transfer the metal liquid to the injection positions. Finally, the ladle moves back to the loading line to continue another round of operations.

According to the practical setup, the transfer mechanism should be designed under the condition that the start loading positions are limited to within the center area of the boiler but multiple injection positions are vertically set in the die-casting machine. Therefore, the synthesis problem studied in this paper is more complex compared to those with only one single manufacturing path [27]. To meet the requirements, the ladle is designed to have an adjustable output bar with multiple modes, in which each mode is set by the bar length

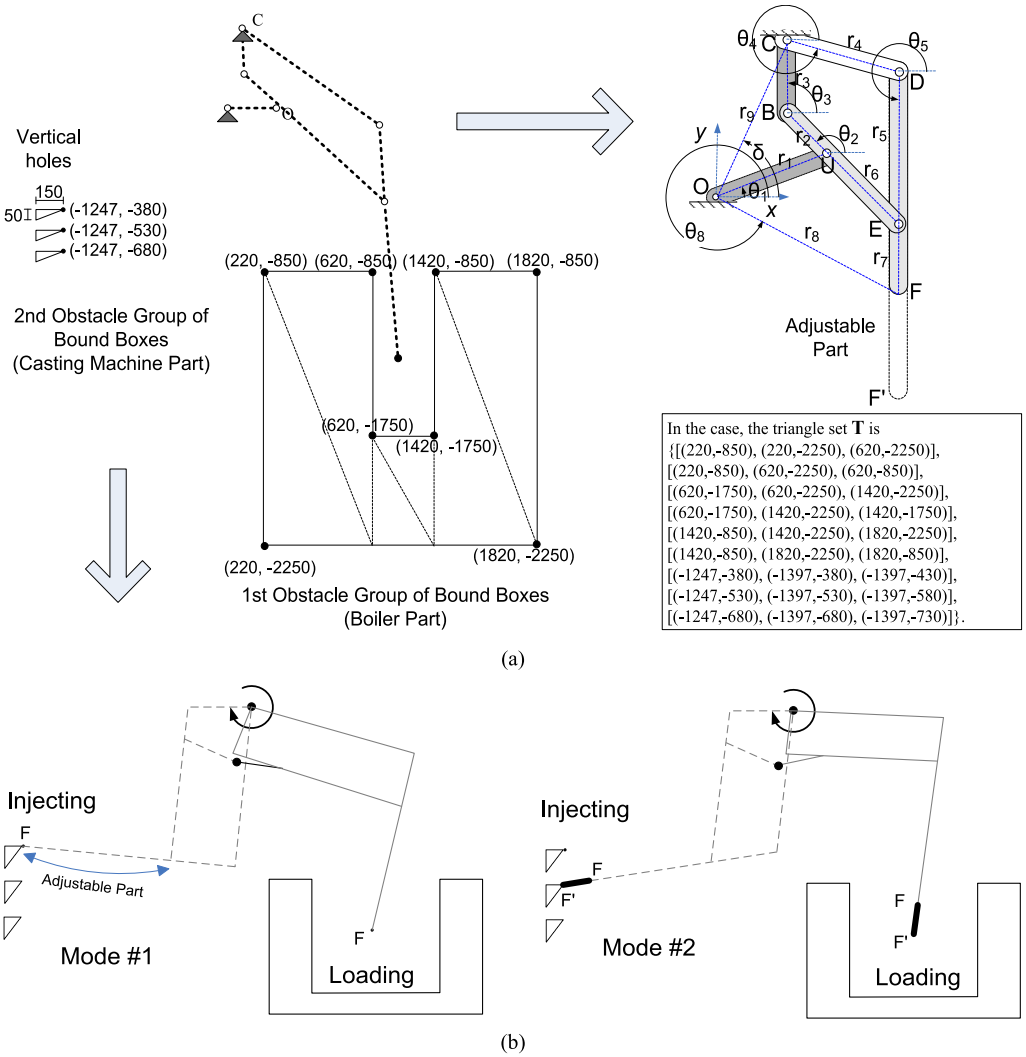

FIGURE 3. Structure of the adjustable six-linkage bar and the locating conditions under different modes. (a) Spatial and structural (draft) designs where F is the ladle end in Mode 1 and F′ is the ladle end in Mode 2. (b) Loading and injection conditions in two different modes.

and the associated input angle. Fig. 3 shows the principle of the structure and locating condition.

To model the collision-free synthesis problem, the kinematic equations of the adjustable ladle mechanism are first analyzed.

A. KINEMATICS ANALYSIS

Suppose that the variable set of fixed-length linkages is $\mathbf{R} = \{r_1, \cdots, r_6\}$, and r_7 is denoted as the base variable of the adjustable bar. In particular, there are d modes in the operation set $\mathbf{D} = \left\{\left(r_{7,\mathrm{i}}, \hat{\theta}_\mathrm{i}, \bar{\theta}_\mathrm{i}\right) | 1 \le i \le d\right\}$ where $r_{7,\mathrm{i}}$ is the length of the adjustable bar, and $\hat{\theta}_\mathrm{i}$ and $\bar{\theta}_\mathrm{i}$ are the initial and final values, respectively, of the input angle in the i-th mode.

When analyzing the structure, pivot O is set as the origin point, and the other parameters can be derived on the basis of the pivot. A complete design should derive the kinematical equations related to the parameters containing the lengths of the linkage bars, the input angle, and the position of the other pivot C.

Although the length of the last bar of the studied linkage mechanism is adjustable, its value is fixed while operating in a specific operation mode. Therefore, we can analyze the kinematical equations of the mechanism operated in a fixed mode. By applying vector loop method for the position analysis of the studied linkage (as shown in Fig. 3(a)), the equations can be formulated as follows:

$$\mathbf{r}_1 + \mathbf{r}_2 = \mathbf{r}_9 + \mathbf{r}_3, \tag{1}$$

$$\mathbf{r}_8 = \mathbf{r}_9 + \mathbf{r}_4 + \mathbf{r}_5 + \mathbf{r}_7, \tag{2}$$

$$\text{and} \quad \mathbf{r}_3 = \mathbf{r}_4 + \mathbf{r}_5 + \mathbf{r}_6 + \mathbf{r}_2. \tag{3}$$

where the notation $\mathbf{r}$ is denoted as a position vector.

Eqs.(1)-(3) can be differentiated to determine the velocities, and the velocity equations can be differentiated again to determine the accelerations.

For example, Eq. (3) can be first rewritten by making use of the unit vectors **i** and **j**:

$$r_4\,(\cos\theta_4\mathbf{i}+\sin\theta_4\mathbf{j})+r_5\,(\cos\theta_5\mathbf{i}+\sin\theta_5\mathbf{j})+(r_6+r_2)\,(\cos\theta_2 i+\sin\theta_2\mathbf{j})-r_3\,(\cos\theta_3 i+\sin\theta_3\mathbf{j}), \quad (4)$$

where r_i is the length of $\mathbf{r_i}, 1 \le \mathrm{i} \le 9$. Then, it can be differentiated to obtain the velocity equations:

$$-r_4\times\omega_4\times\sin\theta_4-r_5\times\omega_5\times\sin\theta_5-(r_6+r_2)\times\omega_2\times\sin\theta_2+r_3\times\omega_3\times\sin\theta_3=0, \quad (5)$$

$$r_4\times\omega_4\times\cos\theta_4+r_5\times\omega_5\times\cos\theta_5+(r_6+r_2)\times\omega_2\times\cos\theta_2-r_3\times\omega_3\times\cos\theta_3=0, \quad (6)$$

where $\omega_\mathrm{i}=\frac{d\theta_\mathrm{i}}{dt}$, $1 \le \mathrm{i} \le 5$. The equations can be differentiated again to obtain acceleration equations.

$$-r_4\times\alpha_4\times\sin\theta_4-r_4\times\omega_4\times\omega_4\times\cos\theta_4-r_5\times\alpha_5\times\sin\theta_5-r_5\times\omega_5\times\omega_5\times\cos\theta_5-(r_6+r_2)\times\alpha_2\times\sin\theta_2-(r_6+r_2)\times\omega_2\times\omega_2\times\cos\theta_2+r_3\times\alpha_3\times\sin\theta_3+r_3\times\omega_3\times\omega_3\times\cos\theta_3=0, \quad (7)$$

$$r_4\times\alpha_4\times\cos\theta_4-r_4\times\omega_4\times\omega_4\times\sin\theta_4+r_5\times\alpha_5\times\cos\theta_5-r_5\times\omega_5\times\omega_5\times\sin\theta_5+(r_6+r_2)\times\alpha_2\times\cos\theta_2-(r_6+r_2)\times\omega_2\times\omega_2\times\sin\theta_2-r_3\times\alpha_3\times\cos\theta_3+r_3\times\omega_3\times\omega_3\times\sin\theta_3=0, \quad (8)$$

where $\alpha_\mathrm{i}=\frac{d\omega_\mathrm{i}}{dt}$, $1 \le \mathrm{i} \le 5$.

The derivation steps above can be applied to Eqs (1) and (2) to obtain the complete equations. Then, we can solve the equations and obtain the position $(p_\mathrm{x}, p_\mathrm{y})$ of the ladle end (F point shown in Fig.3) as follows:

$$p_\mathrm{x}=r_8\times\cos\theta_8=r_9\times\cos\delta+r_4\times\cos\theta_4+(r_5+r_7)\times\cos\theta_8, \quad (9)$$

$$\text{and } p_\mathrm{y}=r_8\times\sin\theta_8=r_9\times\sin\delta+r_4\times\sin\theta_4+(r_5+r_7)\times\sin\theta_8. \quad (10)$$

The acceleration $(a_\mathrm{x}, a_\mathrm{y})$ of the ladle end can be also obtained:

$$\mathrm{A_x}=-r_4\times\alpha_4\times\sin\theta_4-r_4\times\omega_4\times\omega_4\times\cos\theta_4-(r_5+r_7)\times\alpha_5\times\sin\theta_5-(r_5+r_7)\times\omega_5\times\omega_5\times\cos\theta_5, \quad (11)$$

$$\text{and}\quad \mathrm{A_y}=r_4\times\alpha_4\times\cos\theta_4-r_4\times\omega_4\times\omega_4\times\sin\theta_4+(r_5+r_7)\times\alpha_5\times\cos\theta_5-(r_5+r_7)\times\omega_5\times\omega_5\times\sin\theta_5. \quad (12)$$

Finally, the equations of $(p_\mathrm{x}, p_\mathrm{y})$ and $(a_\mathrm{x}, a_\mathrm{y})$ can be derived and organized to be only depended on the variables r_1 to r_7, θ_1, ω_1 and α_1.

B. COLLISION-FREE CONSTRAINTS

During manufacturing operations, the collision-free constraint requires that the manufacturing path should be out of the area covered by the obstacles. In the study, the boiler is an obstacle although it is a manufacturing device; because of the multiple casting-points, the injection part in the metal-mold die-casting machine becomes an additional obstacle when the adjustable linkages perform under the different modes. Therefore, the collision area was modeled as a triangle set **T** which was customized to include the shapes of the boiler and the injection holes according to the practical manufacturing situation. The elements in the set were shown in Fig. 3(a). Furthermore, the manufacturing path was modeled as a trajectory set **J** which contained a group of line segments connecting the trajectory points of the ladle end during the transfer operation. For an expected accurate level γ, it was formulated as $\mathbf{J}=\{\mathrm{J_k}\,|1 \le \mathrm{k} \le \gamma\}$ where $\mathrm{J_k}$ is the k-th line segment $\mathrm{p}^\mathrm{F}_{\mathrm{k}-1}\mathrm{p}^\mathrm{F}_\mathrm{k}$, and $\mathrm{p}^\mathrm{F}_\mathrm{k}$ is the position of ladle end F when the input angle is set to $\hat{\theta}_\mathrm{i}+\mathrm{k}\times(\bar{\theta}_\mathrm{i}-\hat{\theta}_\mathrm{i})/\gamma$ in the i-th mode.

Based on the definitions above, the collision-free constraint function was defined as follows:

$$\eta_\mathrm{i}(\mathbf{R},\mathbf{D},\mathbf{T},\mathbf{J})=\cap_\mathrm{i}(\mathbf{T},\mathbf{J}), \quad (13)$$

where $\cap_\mathrm{i}(.)$ computes the intersection value of the triangles (in **T**) and the line segments (in **J**) in the i-th mode. In particular, the intersection evaluation between triangles and line segments is a classic mathematical problem, and some previous work (e.g. see [28]) has provided program codes for the implementation. In the adjustable linkage design problem, the constraint value should be 0.

C. MANUFACTURING OBJECTIVE

Besides the constraints, the adjustable mechanism should have the capability to accurately locate both the loading and injection positions and to stably perform the transfer operation. Therefore, we defined a step objective function $\phi_\mathrm{i}(\cdot)$ which converted the design objective into a scalar problem by constructing a weight-sum of the acceleration range in the operations and the locating errors at the loading and injection positions. It was formulated as follows:

$$\phi_\mathrm{i}(\mathbf{R},\mathbf{D})=\begin{cases}0, & \alpha_i \le \varepsilon_\alpha,\ \tilde{\mathrm{x}} \le \hat{\varepsilon}_p,\ \tilde{\mathrm{y}} \le \bar{\varepsilon}_p,\\ \tilde{X}-\hat{\varepsilon}_p+\mathrm{y}-\bar{\varepsilon}_p+\beta(\alpha_i-\varepsilon_\alpha), & \text{otherwise},\end{cases} \quad (14)$$

where $\tilde{\mathrm{x}}=\left|\hat{\mathrm{p}}_\mathrm{i}\hat{\mathrm{p}}'_\mathrm{i}\right|$ and $\tilde{y}=\left|\bar{\mathrm{p}}_\mathrm{i}\bar{\mathrm{p}}'_\mathrm{i}\right|$; thresholds $\hat{\varepsilon}_\mathrm{p}$ and $\bar{\varepsilon}_\mathrm{p}$ are the bounds of locating errors; β is the weighting factor between the acceleration and locating error; in the i-th mode, $\alpha_\mathrm{i}=\mathrm{MAX}^\mathrm{l}_{\mathrm{j}=1}\sqrt{a^2_{\mathrm{x,j}}+a^2_{\mathrm{y,j}}}$, and l is the number of the sampling points in the trajectory path; $\hat{\mathrm{p}}'_\mathrm{i}$ and $\bar{\mathrm{p}}'_\mathrm{i}$ are the expected loading and injection positions, and $\hat{\mathrm{p}}_\mathrm{i}$ and $\bar{\mathrm{p}}_\mathrm{i}$ are the actual positions of the ladle end $(p_\mathrm{x}, p_\mathrm{y})$ when the input angles are set to $\hat{\theta}_\mathrm{i}$ and $\bar{\theta}_\mathrm{i}$, respectively.

D. THE OPTIMIZATION PROBLEM

On the basis of these definitions above, the optimal design problem is formulated as follows:

$$\begin{aligned}&\text{Minimize } \mathrm{Max}^\mathrm{d}_{\mathrm{i}=1}\phi_\mathrm{i}(\mathbf{R},\mathbf{D}),\\ &\text{Subject to } \mathrm{Max}^\mathrm{d}_{\mathrm{i}=1}\eta_\mathrm{i}(\mathbf{R},\mathbf{D},\mathbf{T},\mathbf{J})=0,\\ &\qquad \hat{r}_\mathrm{j} \le \mathrm{r_j} \le \bar{r}_\mathrm{j},\ 1 \le \mathrm{j} \le 7,\end{aligned} \quad (15)$$

where $\hat{r}_\mathrm{j}$ and $\bar{r}_\mathrm{j}$ are the customized bounds of $\mathrm{r_j}$.

As formulated in the kinematical equations, some parameters such as the pivot point (C_x, C_y), ω_1, α_1, $\hat{r}_j$ and $\bar{r}_j$ are directly customized by the designer. For the other parameters in the linkage structures, we use the TSCGA to optimize their values.

III. SOLUTION BY USING A TSCGA

Although many state-of-the-art evolutionary algorithms (e.g. [22], [29]–[31]) have been reported to have good capability of exploring a single global optimum, they usually cannot efficiently maintain multiple local or global solutions for optimization problems. In general, the niching methods [32] can be incorporated into a simple EA to efficiently maintain formation of multiple stable subpopulations within a single population. Our previous work [24] thus proposed a crowding method, the twin-space crowding (TSC) method, to dynamically track the niche coverage and remove similar individuals within the niches. TSCGA can maintain a set of diverse solutions and has more promising solution capability compared to the other crowding methods such as the niche crowding GA [33], the deterministic crowding GA [34] and the cluster crowding GA [35].

The pseudo steps of the TSCGA method are summarized as Algorithm 1.

The algorithm steps were detailed in our previous work, and therefore, this paper focuses on the design of the coding schema and the selection of the genetic operators.

A. ENCODING AND DECODING SCHEMAS

In the coding schema, a complete linkage structure is encoded into a chromosome. That is, for a linkage with d-mode operations, the chromosome is encoded as follows:

$$[r_1, \cdots, r_6, r_{7,1}, \cdots, r_{7,d}]. \tag{16}$$

The genes in each chromosome are denoted as the fixed-bar length variables and a group of the adjustable bar length variable in an operation mode.

In the decoding phase, after the structure variables are decoded from the chromosome, a *trajectory evaluation* method is performed to find the best-fitting values for the initial and final angles, $\hat{\theta}_i$ and $\bar{\theta}_i$, of the input angle variable θ_1 in the i-th mode. The pseudo steps are specified as Algorithm 2.

B. GENETIC OPERATORS

Because the selection operation has a strong impact on the diversity of the population and convergence, the tournament selection [25] was used to select chromosomes from the current population for the mating pool. For the crossover, we use simulated binary crossover (SBX) [36]. While using the SBX, the mutation is set up by a mutated value created by a perturbance factor derived from the probability distribution in the SBX and a random value in [0, 1]. These operators were also examined in our previous work [24].

Algorithm 1 The *TSCGA* Algorithm

Main part:

1. Initialize the parent population $\mathbf{P}^0$.
2. Evaluate the fitness of $\mathbf{P}^0$.
3. For t =1 to MAXLOOP
   (1) Perform a tournament selection on $\mathbf{P}^{t-1}$ to select the best-fit individuals for mating pool $\mathbf{M}^t$.
   (2) Perform crossover and mutation operations on $\mathbf{M}^t$ to obtain offspring population $\mathbf{O}^t$.
   (3) Evaluate the fitness of $\mathbf{O}^t$.
   (4) Call the TSC method with the parameters $\mathbf{P}^{t-1}$ and $\mathbf{O}^t$ to obtain population $\mathbf{P}^t$.
4. End

Procedure Part (TSC Method)

Declaration:

Symbol x $\prec$ y denotes that x dominates y if and only if x has a better fitness than y has.
Symbol |xy| denotes the Euclidean distance of x and y in the variable space.
(a) Input:
   (a.1) Parent population $\mathbf{P}=\{P_1, \ldots, P_m\}$ with size m.
   (a.2) Offspring population $\mathbf{O}=\{O_1, \ldots, O_n\}$ with size n.
   (a.3) The dimension number d of any population member.
(b) Output:
   The updated parent population $\mathbf{P}$.

Main part:

1. For $i = 1$ to n
   (1) Find $P' \in \mathbf{P}$ where $\left|P'O_i\right| = \min_{j=1}^{m} \left\{\left|P_jO_i\right|\right\}$.
   (2) If $O_i \prec P'$ then $P' \leftarrow O_i$ and continue (skip to next iteration of loop).
   (3) Compute the set $\mathbf{T} = \left\{T | T' \in \mathbf{P}, \left(\left|T'P'\right| \leq \left|P'O_i\right|\right) \wedge O_i \prec T'\right\}$.
   (4) If $\mathbf{T} <> \emptyset$ then
      (4.1) Define a variable Q where $Q_j = \frac{O_{i,j}+P'_j}{2}$, $1 \leq j \leq d$.
      (4.2) If $Q \prec P'$ then $P' \leftarrow Q$ and continue.
      (4.3) If $Q \prec O_i$ then continue.
      (4.4) Randomly choose a member $\bar{T}$ from $\mathbf{T}$, and $\bar{T} \leftarrow O_i$.
   (5) End if
2. End for

C. FITNESS EVALUATION

For each chromosome, the fitness is evaluated from the objective equation of the optimization problem specified in Eq. (15). Because a tournament selection is adopted, the fitness does not need to be scaled as is required in a proportional selection, such as the roulette-wheel method. Instead, a constraint dominance relation [37] is used to cooperate

Algorithm 2 Trajectory Evaluation (for the i-th Mode)

Declaration

(a) Input:

(a.1) the length variables $r_1, \cdots, r_6, r_{7,i}$.

(a.2) the loading and injection positions $\hat{p}'_i$ and $\bar{p}'_i$.

(b) Output:

the input angles $\hat{\theta}_i$ and $\bar{\theta}_i$ in the loading and injection positions.

Main part:

1. Compute the minimal locating error at the start angle:

$$\mathrm{MIN}_{\theta_1=\hat{\theta}}^{\theta_1=\bar{\theta}} \left|\hat{p}'_i p_i\right|, \tag{17}$$

where $\hat{\theta}$ and $\bar{\theta}$ are the bounds of the input angle θ_1, $\hat{p}'_i$ is the expected loading position, and p_i is the actual position of the ladle end at θ_1 in the i-th mode. Record the input angle as $\hat{\theta}_i$ in the minimal condition.

2. Compute the minimal locating error at the end angle:

$$\mathrm{MIN}_{\theta_1=\hat{\theta}_i}^{\theta_1=\bar{\theta}} \left|\bar{p}'_i p_i\right|, \tag{18}$$

where $\hat{\theta}_i$ is obtained in the first step, and $\bar{p}'_i$ is the expected injection position. Record the input angle as $\bar{\theta}_i$ in the minimal condition.

with the selection. In the dominance evaluation between two chromosomes, constraint violations are first compared; the objective values are then compared if the violations are the same. The superior one is chosen in the tournament selection.

IV. EXPERIMENTS AND DISCUSSION

The proposed GA flow to solve the linkage design problems is shown in Fig. 4. To verify the solution capability of the proposed approach, the synthesis of adjustable four-linkage bars for function generation problems in the literature is first studied. In the case, the fitness functions are designed to include the expected design variables and objective according to the problem requirements in the work of Zhou [8]. Then, the proposed approach is used to solve the practical collision-free design problem of an adjustable six-bar ladle for a metal-mold die-casting system.

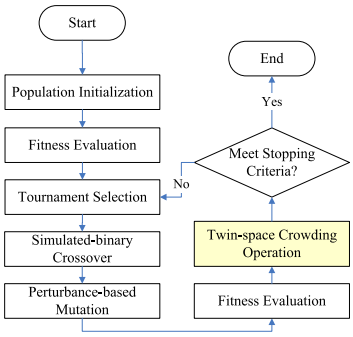

FIGURE 4. Flow chart of the TSCGA.

A. OPTIMAL FUNCTION GENERATION OF ADJUSTABLE LINKAGE BARS

The function generation problem is specified as follows: function $f(x) = y$ is to be generated by a linkage in a certain range of x; the input and output angles of the linkage need to be proportionally related to the variables x and y, respectively. Because the function generated by a four-linkage bar can only match the expected function at limited precise points, an adjustable linkage structure is used. Fig. 5 shows the principle design of Zhou [8], which includes an assistant bar to adjust the pivot position. This design contains two additional bars and a passive bar, forming a local parallelogram to transfer the output rotation.

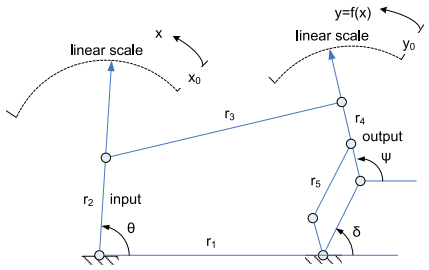

FIGURE 5. Adjustable linkage for function generation (Zhou, 2008).

For the adjustable linkage to properly generate the desired function, some parameters must be properly synthesized by the designer. The independent design variables are denoted as follows:

$$[\theta_0, \varphi_0, r_1, r_3, r_4, r_5], \tag{19}$$

where θ_0 and φ_0 are the initial input and output angle values respective to the variables x_0 and y_0 as shown in Fig. 5, and the length of the input link r_2 is set to 1. For the entire x range, the required value of the adjustable angle δ is computed and used to transfer the pivot position for perfect function generation. The range $\Delta\delta$ is the optimization objective and can be calculated from the required maximum and minimum δ values

$$\text{Minimize } (\delta_{\max} - \delta_{\min}). \tag{20}$$

The kinematic equations related to the structure are detailed in Norton [39] and Zhou [8].

In the work of Zhou [8], a local optimum solver, the constrained nonlinear minimization algorithm *fmincon*, in the optimization toolbox of MATLAB was used to optimize the synthesis problem. In this paper, the TSCGA was used to explore a global solution for the same optimization problem. Two synthesis examples, the *sin* function and the *log* function were studied. In the *sin* function, the desired function was $y = sin(x)$ over $0° \leq x \leq 90°$. The input and output rotation ranges were specified as $\Delta\theta = 120°$ and $\Delta\varphi = 60°$. The genetic parameters in this case were a parent number of 100, an offspring number of 80, a crossover rate of 1.0,

a mutation rate of 0.1, and an evolutionary loop count limited to within 5000.

TABLE 1. Synthesis results of function *sin*(*x*) generation.

Method	No	Function *sin*(*x*)						
		$\Delta\delta$	θ_0	φ_0	r_1	r_3	r_4	r_5
Zhou [8]	-	0.13983	98.4592	90.694	4	2.16817	1.279	2.01525
TSCGA (This work)	#1	0.10578	100.28468	91.42602	3.83998	2.35078	1.28534	1.74015
	#2	0.10016	101.01138	91.44431	3.99684	2.49039	1.29059	1.81041
	#3	**0.07586**	**105.78935**	**96.68521**	**3.96768**	**2.37803**	**1.28583**	**1.93218**
	#4	0.13449	104.85145	96.17238	3.38559	2.23842	1.27841	1.43796
	#5	0.13500	107.87245	95.09018	3.74166	2.84774	1.30674	1.60108
	#6	0.10551	107.65888	97.9862	2.94533	2.48046	1.28999	1.01501
	#7	0.11153	107.95051	95.62073	3.80296	3.33061	1.32233	1.56273
	#8	0.11910	107.73026	96.8235	2.98982	2.78955	1.30115	1.02461
	#9	0.12251	106.8488	94.59126	3.32502	3.20743	1.31722	1.21504
	#10	0.11730	107.02967	93.19484	3.94684	3.80871	1.34037	1.65023
	#11	0.1147	107.03716	92.97291	4	3.89952	1.34316	1.69457
	#12	0.11630	107.87437	93.9645	3.99518	3.96801	1.34447	1.75955
	#13	0.11987	107.88809	93.99408	3.93232	3.97599	1.34468	1.73634
	#14	0.12718	107.77738	94.39757	3.46067	3.65769	1.33397	1.44729
	#15	0.13439	106.46111	92.52342	3.56349	3.85627	1.34154	1.48153
	#16	0.13028	107.97905	94.11402	3.56943	3.90002	1.34245	1.59319

TABLE 2. Synthesis results of function *log*(*x*) generation.

Method	No	Function *log*(*x*)						
		$\Delta\delta$	θ_0	φ_0	r_1	r_3	r_4	r_5
Zhou [8]	-	0.04896	118.814	55.9654	2.25888	2.38282	1.18608	1.40852
TSCGA (This work)	**#1**	**0.02606**	**127.28107**	**60.82933**	**3.30274**	**2.33912**	**1.19938**	**2.53742**
	#2	0.03762	127.86685	52.8578	2.53406	2.37852	1.33707	1.89198
	#3	0.03676	125.86244	50.95403	2.40882	2.35214	1.29789	1.72671
	#4	0.04418	121.18706	51.5732	2.55034	2.35252	1.26635	1.76965
	#5	0.033	123.9622	63.38918	3.10969	2.41788	1.16909	2.25605
	#6	0.04594	127.99807	60.63468	2.32338	2.37761	1.29409	1.71653
	#7	0.04116	124.46075	55.27157	2.10999	2.32894	1.22261	1.40422
	#8	0.04198	124.79219	58.10156	2.12897	2.34082	1.20699	1.42644

*Remark: The smaller $\Delta\delta$ is better.

TABLE 3. Setup parameters in the design problem of the six-bar ladle.

Parameter	Value	Vertices of the Obstacles
β	1000	Boiler shape (split rectangles):
ω_1	0.01 (rad/sec)	#1: (220,-850), (220,-2250), (620,-2250), (620,-850)
α_1	0 (mm/sec2)	#2: (620,-1750), (620,-2250), (1420,-2250),(1420,-1750)
$\hat{\varepsilon}_p$	5cm	#3: (1420,-850),(1420,-2250), (1820,-2250),(1820,-850)
$\bar{\varepsilon}_p$	5mm	#4: (-1250,-2250),(-1250,0), (-1350,0),(-1350,-2250)
ε_α	0.5 mm/sec^2	
γ	360	
(C_x, C_y)	(122.5, 495.7)	
$[\hat{r}_1, \bar{r}_1]$	[200, 800]	Injection-hole shapes (triangles):
$[\hat{r}_2, \bar{r}_2]$	[200,800]	#1: (-1247,-380), (-1397,-380), (-1397,-430)
$[\hat{r}_3, \bar{r}_3]$	[200,800]	#2: (-1247,-530), (-1397,-530), (-1397,-580)
$[\hat{r}_4, \bar{r}_4]$	[1200, 1800]	#3: (-1247,-680), (-1397,-680), (-1397,-730)
$[\hat{r}_5, \bar{r}_5]$	[200,800]	
$[\hat{r}_6, \bar{r}_6]$	[700,1300]	
$[\hat{r}_7, \bar{r}_7]$	[700,1300]	

1) SOLUTION MULTIPLICITY

Tables 1 and 2 lists the synthesis results of the desired functions, which contain the parameters of the linkage structures explored by the local optimization method and the TSCGA. From the tables, the local optimization method only found a single solution while generating either *sin* or *log* function but

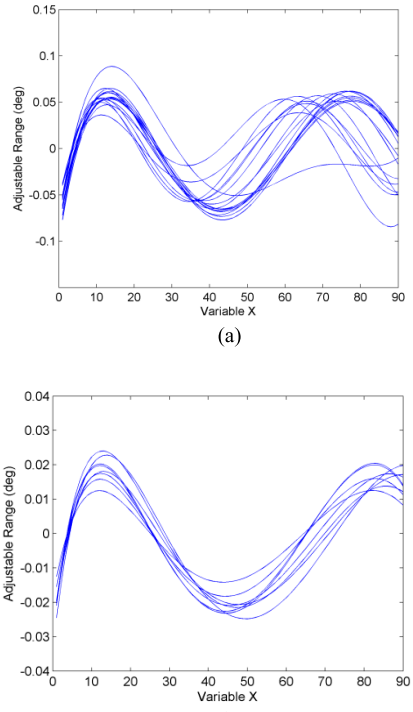

FIGURE 6. Various adjustment curves of δ values explored by the TSCGA method. (a) Adjustments in the function generation of *sin*(*x*). (b) Adjustments in the function generation of *log*(*x*).

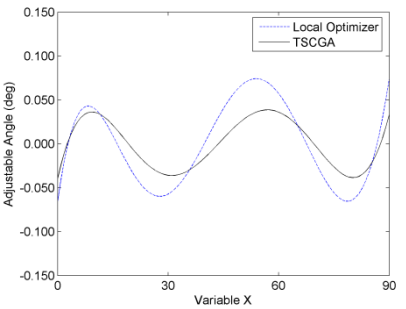

FIGURE 7. Variation of δ values of solution #3 in the function generation of *sin*(*x*) explored by the TSCGA method.

the TSCGA can explore more solutions by maintaining a set of population with diversity.

Fig. 6 shows the adjustment curves of δ in the explored solutions of the TSCGA. In the two function generation problems, the solutions of TSCGA dominate those of the local optimization method. As shown in Tables 1 and 2, there are total 16 designs explored while generating the *sin* function, and in the *log* function, 8 designs are obtained. These distinct solutions can be used for the final design choice.

2) PRECISE SYNTHESIS

Besides the solution multiplicity, the TSCGA can obtain more precise solutions. In the *sin* function, the optimal adjustment range in the local solution was 0.13983; the solution #3 by the TSCGA improves this to 0.07587, or approximately 54% of

TABLE 4. Synthesis result of vertical-direction holes.

NO	r_1 (mm)	r_2 (mm)	r_3 (mm)	r_4 (mm)	r_5 (mm)	r_6 (mm)	$r_{7,1}(\bar{\theta}_1, \bar{\theta}_1)$ mm(deg,deg)	$r_{7,2}(\bar{\theta}_2, \bar{\theta}_2)$ mm(deg,deg)	$r_{7,3}(\bar{\theta}_3, \bar{\theta}_3)$ mm(deg,deg)
#1	334.3	325.6	381.3	523.9	1354.7	1295.5	895.5(-7,148.5)	1053.5(0,137)	1246.3(8.5,125.5)
#2	329.7	300.2	335	394.1	1293.9	1252.6	779(-4,146)	957.2(3.5,135.5)	1127.5(10,126.5)
#3	333.9	322.9	330	403.9	1293.9	1270.7	740.6(-6.5,148)	900.3(0,137)	1057.2(7,127.5)
#4	334.7	341.5	364.6	439	1278.4	1259.6	830.5(-8.5,150.5)	954(-3,140)	1091(3.5,131)
#5	335.9	317.1	387	476.2	1282.8	1234.4	874.5(-8.5,150.5)	1017.2(-2.5,140)	1176.1(4.5,130.5)
#6	336.4	297.4	352.8	450.5	1391.3	1301.9	778.9(-5.5,148.5)	956.9(1,138.5)	1126.8(7.5,129.5)
#7	333.2	352.4	377.3	398.5	1281.3	1270.4	871.2(-8.5,150.5)	975.4(-3.5,141.5)	1086(1.5,133.5)
#8	338.2	305.5	390	524.2	1354.7	1273.5	895.1(-7,149)	1053.5(-1,138.5)	1246.4(7.5,128)
#9	338.2	364.3	391.4	423.6	1291	1282.4	878.5(-10,152)	975.4(-6,143)	1086(-0.5,135)
#10	333.5	310.4	329.7	437.7	1346.3	1294.8	738.7(-5,147.5)	918.7(2,136)	1099.8(9.5,126)
#11	328.8	292.1	326.8	372.1	1242.7	1210.8	748.9(-4,146.5)	930.7(3.5,135.5)	1097.1(10,126.5)
#12	335.1	321.7	385	458.8	1282.5	1239.1	866(-9,151)	1012.9(-2.5,140.5)	1152.2(4,131.5)
#13	333.9	320.6	339.5	443.3	1310.2	1272.4	762.4(-6.5,149)	925.9(0,137.5)	1093(7.5,127.5)
#14	341	314.1	352.7	425.9	1315.8	1261.9	740.6(-9,151)	900.3(-2.5,140.5)	1057.2(4,131.5)
#15	335.4	365.4	415.1	475.3	1291	1282.8	945(-10,151.5)	1054.1(-5,141.5)	1179(1,132.5)
#16	333.7	332.5	377.3	397.7	1282.3	1250.5	859.7(-8.5,150.5)	976(-3,142)	1095.6(2,134)
#17	344.9	320.5	382.2	519.6	1375.6	1289.9	801.7(-10,153)	957.2(-4.5,142)	1124.9(2.5,132)
#18	329.4	303	324.7	366.8	1293.9	1253.1	743.8(-4,146.5)	900.3(2,137)	1067.9(9,128)
#19	334.5	318.2	339.5	471.8	1310.2	1269.7	756(-6.5,149)	925.9(0,137)	1117.8(8.5,125.5)
#20	332.8	302	330.3	403.7	1293.8	1249	718.9(-5.5,148.5)	904.9(1.5,137)	1080.2(8.5,127.5)
#21	336	328.9	412.4	426.4	1195.5	1180	937.1(-10,152)	1037.8(-5,143)	1156.2(0.5,134.5)
#22	330.3	304.5	342.8	366.8	1293.9	1246.6	791.5(-5,147.5)	933.5(1,138.5)	1072.7(6.5,131)
#23	330.2	301.4	330.1	389.9	1294.6	1251.1	744.7(-5,147.5)	923.7(2.5,136.5)	1088.2(9,127.5)
#24	337.5	308	394	489.8	1365.6	1282.9	894.7(-8,150)	1053.5(-1.5,140)	1213.7(5,131)
#25	330.1	300.6	330.1	391.4	1293.9	1252.4	762.4(-4,146.5)	925.9(2.5,136)	1103.5(10,126.5)
#26	335.1	329.7	362.5	450.5	1393.6	1334.3	837.1(-7,148.5)	982.3(-0.5,138.5)	1128.9(5.5,130)
#27	342.9	342.7	352.7	442.5	1393.6	1336.2	746.3(-10,151.5)	884.3(-4.5,142)	1027.6(1.5,133)
#28	334.3	336.4	339.2	443.3	1310.2	1288.2	762.1(-7.5,149)	914.2(-1,138)	1083.6(6.5,127)
#29	330.3	315.6	324.7	366.8	1294.1	1265.5	743.8(-5.5,147)	900.3(1.5,137)	1050.6(8,128.5)
#30	335.7	352.4	340.2	384.7	1208.5	1222.1	765.1(-10,151.5)	864.8(-5,141.5)	986.8(1,132.5)
#31	333.9	306.7	329.7	436.3	1346.3	1291.4	727.7(-5,147.5)	920.2(2,136)	1103.5(9.5,126)
#32	334	381.1	409.9	465.5	1355.4	1347.3	953.6(-9,150)	1054.1(-4,141)	1179(2,132)

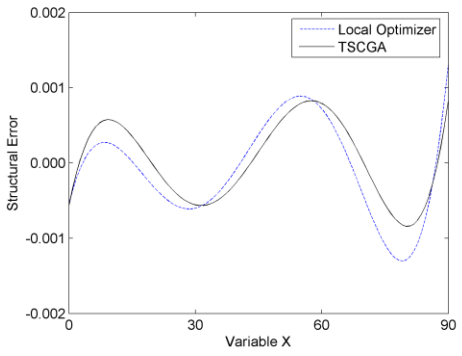

FIGURE 8. The structural errors in the function generation of *sin*(*x*) with a fixed δ.

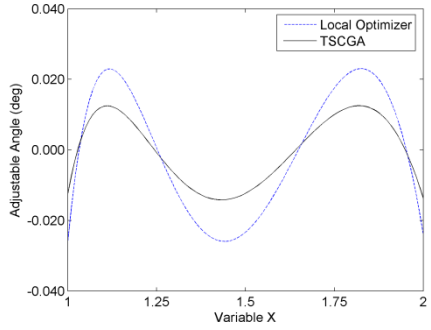

FIGURE 9. Variation of δ values in the optimal function generation of *log*(*x*) explored by the TSCGA method.

the local solution range. The required continuous adjustments of δ in the TSCGA solution #3 for the exact synthesis problem are shown in Fig. 7. If a fixed pivot is used, then an exact

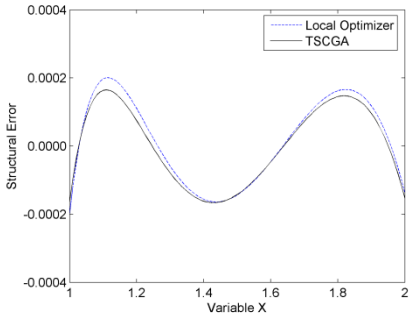

FIGURE 10. The structural errors in the function generation of *log*(*x*) with a fixed δ.

synthesis cannot be obtained, and a structural error will occur. However, as shown in Fig. 8, the optimal structural error based on a fixed-pivot rule in the local optimum method is 0.00131, which is occurred at the pivot value of $\delta = 175.69°$, and the value was also improved to 0.00084 by setting a fixed pivot of $\delta = 164.54°$.

In the *log* function, the desired function was $y = log(x)$ over $1 \leq x \leq 2$. The input and output rotation ranges were specified as $\Delta\theta = 60°$ and $\Delta\varphi = 60°$. Table 2 lists the synthesis result of the desired function. Fig. 6(b) shows the adjustments of δ in all the solutions. In particular, the optimal adjustment range of the local optimization method was 0.04896, and the value is improved to 0.0267 by the TSCGA. The required continuous adjustments of δ in the TSCGA solution #1 for the exact synthesis are shown

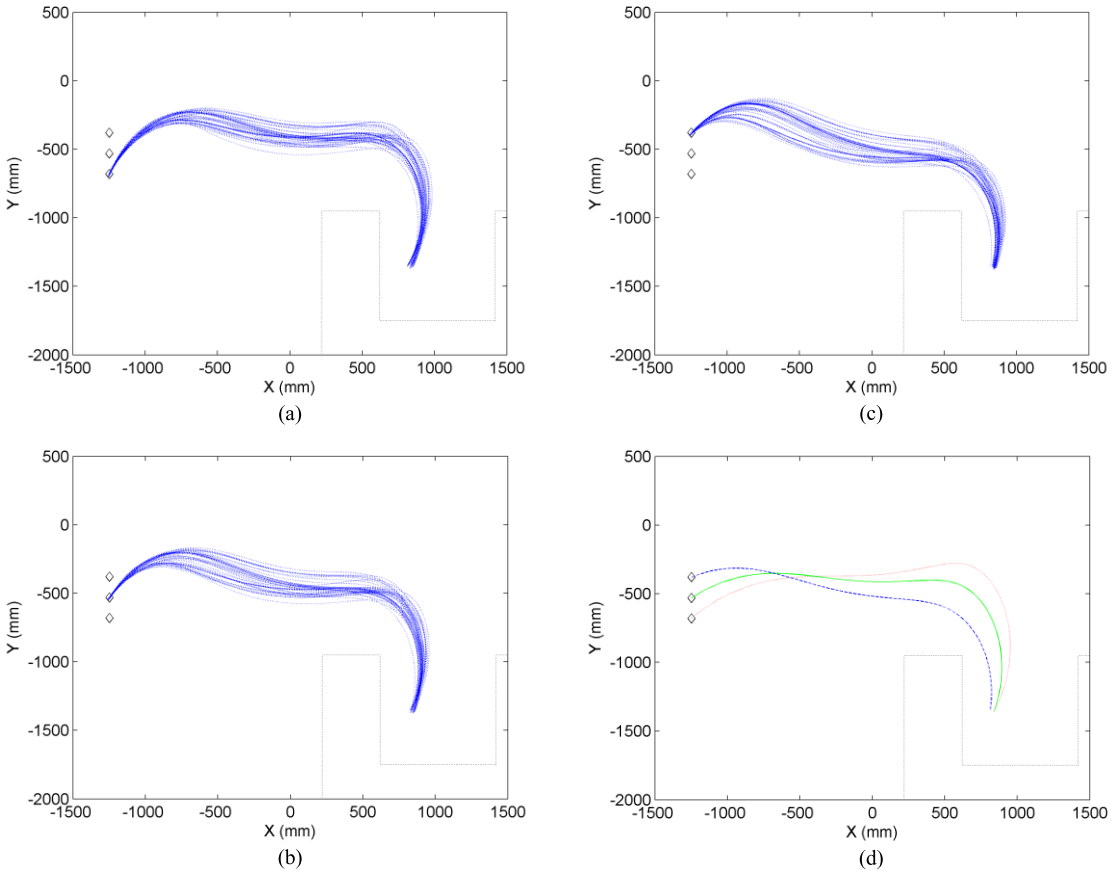

FIGURE 11. Multiple synthesis designs explored by the TSCGA. (a) All the transferring paths in mode 0. (b) All the transferring paths in mode 1. (c) All the transferring paths in mode 2. (d) Transferring paths of solution #1 in the three modes.

in Fig. 9. Fig. 10 shows the structural errors generated by the two methods if the fixed-pivot rule is considered.

In these two examples, the TSCGA method obtained superior results compared to the local optimization method.

B. COLLISION-FREE SYNTHESIS OF THE SIX-LINKAGE BAR STRUCTURE

In the case study, there were three modes to be considered; that is, $d = 34$, as shown in Fig. 3. The loading position was (838, −1350), and in the practice, the error allowance range for position locating was limited within 5cm. The positions of the injection holes were vertically set to (−1247, −380), (−1247, −530), and (−1247, −680), but the error allowance range for position locating was limited to 0.5cm. The other design parameters are summarized in Table 3. The genetic parameters specified in the previous section were also adopted in this case study expect that the execution loop count was set to 50000.

1) SOLUTION MULTIPLICITY IN THE SIX-BAR DESIGN PROBLEM

Table 4 displays the result of the TSCGA, which contains 32 optimal solutions. All the solutions meet the collision-free constraints and have the minimal objective values. The transferring paths in the different modes are shown in Fig. 11. These manufacturing curves are diversely distributed in the space.

Based on the solutions, designers have more references to choose the final design. In general, the designer can select a final design through coupling refinements, for example, adjusting the parameter range or increasing additional constraints.

2) MANUFACTURING PATHS IN THE DESIGN

The simulated execution of solution #1 is shown in detail: its manufacturing paths for the operation modes are shown in Fig. 11(d), in which each path is outside of the obstacle area; in the solution, the values of pairs $(r_7, \hat{\theta}, \bar{\theta})$ are (895.5mm, −7°, 148.5°), (1053.3mm, 0°, 137°) and (1246.3mm, 8.5°, 125.5°) in the three modes; the ladle end reached the three loading areas within a circular range of 5 cm radius, and located the three injection holes within a position error of 0.5 cm; the solution satisfied the design requirement.

Furthermore, all the acceleration values during operations were within the limited range, and the maximal acceleration value occurred in the third mode with a value of 0.313 mm/sec^2. The operation paths and its relative acceleration diagrams are shown in Fig. 12.

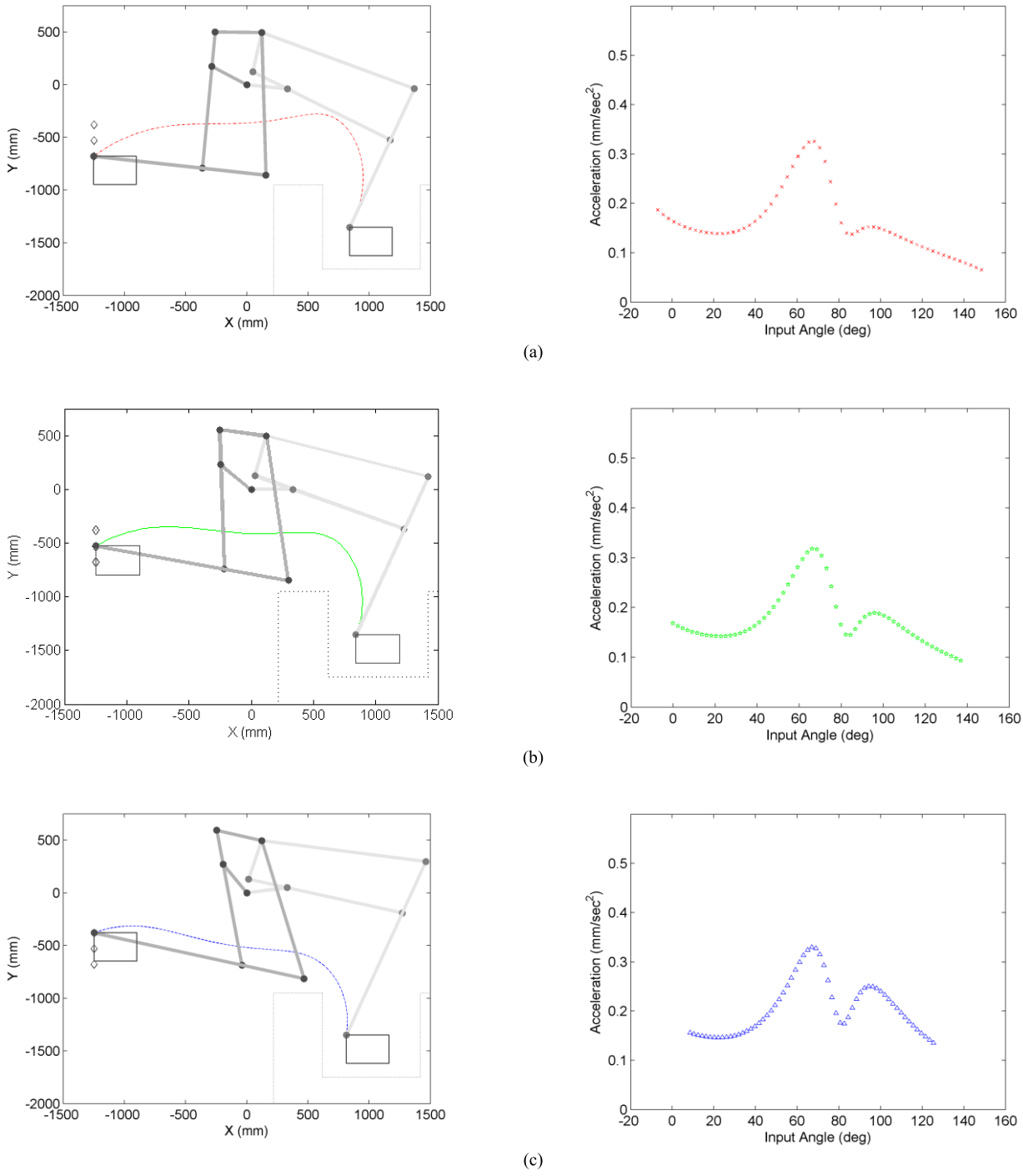

FIGURE 12. Transfer operation and the related acceleration diagram in the vertical- direction hole case. (a) Transferring path and acceleration variations in Mode 1. (b) Transferring path and acceleration variations in Mode 2. (c) Transferring path and acceleration variations in Mode 3.

3) SCALABILITY VERIFICATION OF THE PROPOSED APPROACH

Another injection arrangement was used to verify the scalability of the proposed approach. A horizontal arrangement was considered here, in which the loading position was also set to (838, −1350), but the injection positions were set to (−947, −680), (−1097, −680) and (−1247, −680).

Using the same genetic parameters, the result is shown in Table 5. Fig. 13 shows the manufacturing curves of these solutions. In particular, in solution #1, the values of pairs $(r_7, \hat{\theta}, \bar{\theta})$ are (1025.6mm, 2°, 142.5°), (879.6mm, −4.5°, 142°), and (751.1mm, −10°, 140.5°), separately. Fig. 14 shows the manufacturing paths and its acceleration variations diagram under the

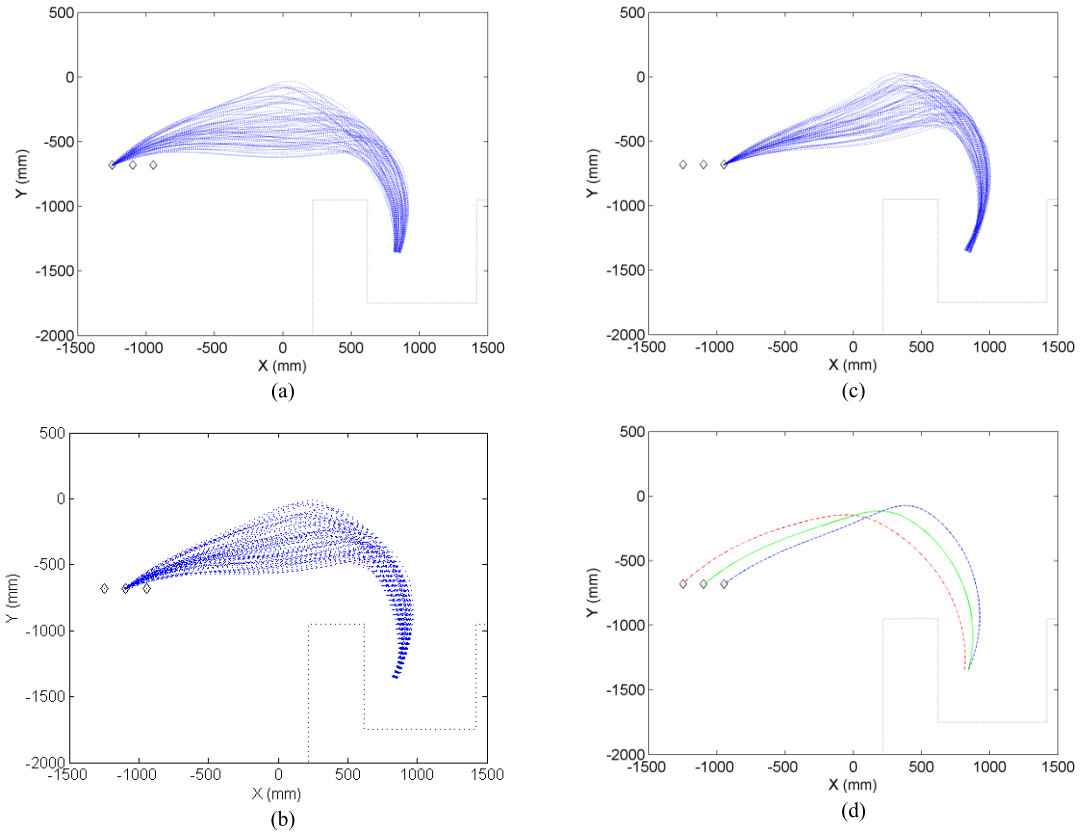

FIGURE 13. Transferring paths under different modes for the horizontal-direction holes. (a) All the transferring paths in mode 0. (b) All the transferring paths in mode 1. (c) All the transferring paths in mode 2. (d) Transferring paths of solution #1 in the three modes.

TABLE 5. Synthesis result of horizontal-direction holes.

NO	r_1 (mm)	r_2 (mm)	r_3 (mm)	r_4 (mm)	r_5 (mm)	r_6 (mm)	$r_{7,1}(\hat{\theta}_1, \bar{\theta}_1)$ mm(deg,deg)	$r_{7,2}(\hat{\theta}_2, \bar{\theta}_2)$ mm(deg,deg)	$r_{7,3}(\hat{\theta}_3, \bar{\theta}_3)$ mm(deg,deg)
#1	307.8	305.6	371.1	393.8	1318.2	1274.7	1025.6(2,142.5)	879.6(-4.5,142)	751.1(-10,140.5)
#2	308	287.8	386.9	532.2	1316.9	1257.8	1163.1(6.5,136.5)	1032.5(0.5,135.5)	898.7(-5,134.5)
#3	308.2	306.7	367.4	436.9	1373.4	1323	1056.2(4,139.5)	921.6(-2,138.5)	795.2(-7.5,137)
#4	309.4	279.4	379.8	529	1231.9	1201	1175.3(8,134)	1031.7(1.5,133.5)	889.6(-4.5,133)
#5	313	311.9	390.7	533.8	1394.3	1319.7	1080.7(1,142)	946.9(-4.5,140.5)	828.7(-9.5,138.5)
#6	304.3	266.4	386.8	461.4	1324.1	1254.1	1177.8(7.5,137)	1049.8(2,136)	924.7(-3,134.5)
#7	313.2	271.2	359.4	532.2	1297	1237.8	1060.8(6,136)	940(1,134.5)	814(-3.5,133.5)
#8	305.6	343.6	367.4	448.3	1372.9	1360.4	1056.4(3.5,139)	930.2(-2.5,137)	800.7(-9,135.5)
#9	307.8	301	372.4	393.6	1290.9	1250.3	1025.6(1.5,142.5)	879.4(-4.5,142)	751.1(-10,140.5)
#10	312.8	282	345.9	421.8	1213.8	1196.1	969.4(3.5,139)	825.8(-2.5,138.5)	693.6(-7.5,137.5)
#11	302.3	294.5	398.4	532.2	1316.9	1264.8	1233(8,135.5)	1089.5(1.5,135)	963.2(-4,133.5)
#12	315	283.8	352.2	400.7	1368.7	1297	950.4(2.5,141.5)	819.5(-3,140)	707.6(-7,138)
#13	314.4	263.3	383.1	501.1	1239.5	1184.3	1090(4,139)	944.8(-2,138.5)	805.1(-7,138)
#14	313.8	343.6	348.9	436.9	1373.5	1358.6	950.4(0.5,141)	819.5(-5.5,139.5)	705.9(-10,137)
#15	314.5	297.9	348.9	436.9	1373.5	1312.2	949.6(2,141)	819.5(-3,139.5)	707.6(-7.5,137.5)
#16	302.4	283.4	383.8	411.4	1259.1	1221.4	1132.6(5.5,139)	983.2(-1,138.5)	844.8(-7,138)
#17	311.8	301.3	394.7	533.8	1394.3	1322	1145.8(4,139)	1013.5(-2,137.5)	898.7(-7,135.5)
#18	315.8	285.4	352.1	436.9	1373.5	1299.7	949.6(2,141.5)	819.5(-3,140)	707.6(-7,138)
#19	305.5	263.4	386.8	461.4	1324.1	1251.1	1177.8(7.5,137)	1048.3(2,136)	904.8(-3.5,135.5)
#20	312.2	285.2	361.9	532.2	1295.3	1253.8	1096.7(7,134.5)	972.7(1.5,133)	844.8(-3.5,132)
#21	313.1	282	344.1	470.8	1373.3	1304.5	978.1(5,138)	869(0.5,136)	752.6(-3.5,134)
#22	302.5	300.9	368.4	443.7	1366	1320.3	1119.3(7,136.5)	1002.2(2,135)	871.6(-3.5,133.5)
#23	307.8	301	374.7	468.3	1237.9	1221.9	1090(4.5,138)	944.8(-2.5,138)	797.2(-9,137.5)
#24	314.3	285.5	382.5	532.2	1295.3	1242.1	1094.7(3.5,138.5)	969.9(-2,137)	837.5(-7,136)
#25	308	248.5	368.5	439.9	1315.8	1233.9	1096.5(7.5,137)	969.9(2.5,136)	836.7(-2,135)
#26	306.6	340.3	343.4	373.7	1373.5	1353.6	959(2,141.5)	819.5(-4.5,140.5)	699.2(-10,138)
#27	313.2	261.2	379.3	531.7	1295.3	1216.8	1096.1(5,138)	973(0,137)	836.8(-5,136)

different modes. The maximal acceleration value in this case occurred in the third mode with a value of 0.251 mm/sec^2.

To sum up, the proposed approach can successfully solve synthesis design problems with the multiplicity of solutions, and each mechanism in the design solution can perform

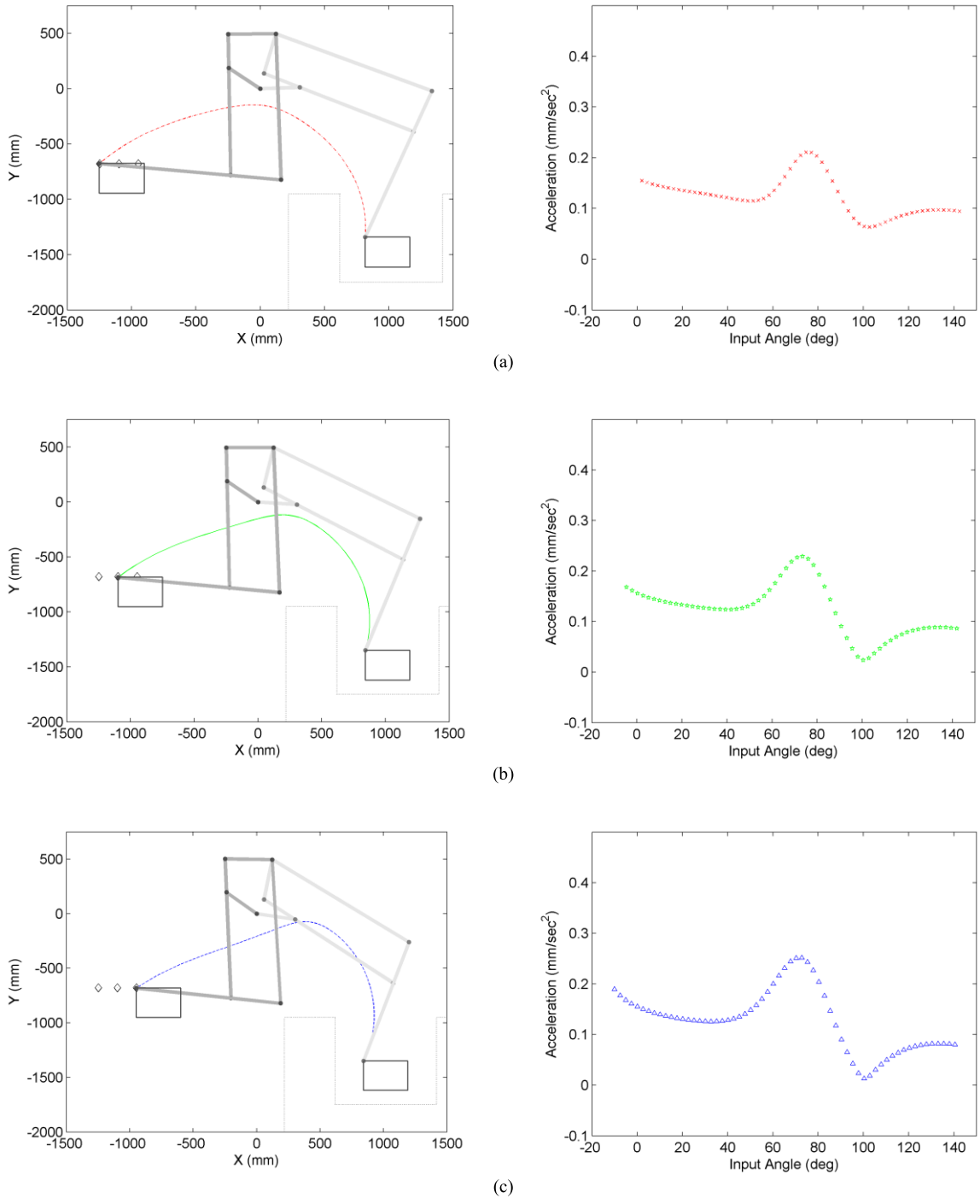

FIGURE 14. Transfer operation and the related acceleration diagram in the horizontal-direction hole case. (a) Transferring path and acceleration variations in Mode 1. (b) Transferring path and acceleration variations in Mode 2. (c) Transferring path and acceleration variations in Mode 3.

precise loading and injection operations in multiple collision-free manufacturing paths.

V. CONCLUSIONS

In this paper, we used the TSCGA to solve the optimal synthesis of collision-free adjustable six-linkage bars with multiple-operation modes. By formulating the collision-free issue as the constraints and including the kinematical requirements into the fitness evaluation, the proposed approach successfully explored multiple design solutions which synthesized the required different manufacturing paths for the six-linkage bar ladle mechanism, and could precisely locate a single loading position and multiple injection holes with an adjustable bar.

Furthermore, this paper studied an adjustable four linkage-bar structure that was discussed in the literature. Compared to the local optimization solutions, the proposed evolutionary approach could obtain superior and more precise synthesis results.

Extensions of this work may contain scalability validations for different design requirements of adjustable linkages. For example, the adjustable part is changed to another link or a movable pivot is included as another design variable. The reasoning formulation can be also extended or modified to include multiple design objectives and additional constraints. However, it requires a well-designed multiobjective optimization method to serve as a solver.

Now, the Technology Base Corporation (TBC) (http://www.tbc-diecast.com/company.htm) has already been licensed to use the proposed design method to find the optimal synthesis design of adjustable six-linkage mechanisms in metal-mold die-casting systems.

ACKNOWLEDGMENT

The authors thank Technology Base Corporation, a professional manufacturing auto-ladler manufacturing company, for their help during this research.

REFERENCES

[1] G. H. Martin, *Kinematics and Dynamics of Machines*. New York, NY, USA: McGraw-Hill, 1982.

[2] K. J. Waldron and G. L. Kinzel, *Kinematics, Dynamics, and Design of Machinery*. New York, NY, USA: Wiley, 2004.

[3] X. Liang, Y. Ding, Z. Wang, K. Hao, K. Hone, and H. Wang, "Bidirectional optimization of the melting spinning process," *IEEE Trans. Cybern.*, vol. 44, no. 2, pp. 240–251, Feb. 2014.

[4] S. Wilhelm and J. Van de Ven, "Adjustable linkage pump: Efficiency modeling and experimental validation," *J. Mech. Robot.*, vol. 7, no. 3, p. 031013, 2015.

[5] D. C. Tao and S. Krishnamoorthy, "Linkage mechanism adjustable for variable symmetrical coupler curves with a double point," *Mech. Mach. Theory*, vol. 13, no. 6, pp. 585–591, 1978.

[6] A. Ahmad and K. J. Waldron, "Synthesis of adjustable planar 4-bar mechanisms," *Mech. Mach. Theory*, vol. 14, no. 6, pp. 405–411, 1979.

[7] D. P. Naik and C. Amarnath, "Synthesis of adjustable four bar function generators through five bar loop closure equations," *Mech. Mach. Theory*, vol. 24, no. 6, pp. 523–526, 1989.

[8] H. Zhou, "Synthesis of adjustable function generation linkages using the optimal pivot adjustment," *Mech. Mach. Theory*, vol. 44, no. 5, pp. 983–990, 2009.

[9] G. Ganesan and M. Sekar, "Kinematic analysis of rectangular path generating adjustable four-bar linkage," *Appl. Mech. Mater.*, vols. 592–594, pp. 1094–1098, Jul. 2014.

[10] B. Hong and A. G. Erdman, "A method for adjustable planar and spherical four-bar linkage synthesis," *J. Mech. Design*, vol. 127, no. 3, pp. 456–463, 2005.

[11] R.-C. Soong and S.-B. Chang, "Synthesis of function-generation mechanisms using variable length driving links," *Mech. Mach. Theory*, vol. 46, no. 11, pp. 1696–1706, 2011.

[12] H. Shimojima, K. Ogawa, A. Fujiwara, and O. Sato, "Kinematic synthesis of adjustable mechanisms: Part 1, Path generators," *Bull. JSME*, vol. 26, no. 214, pp. 627–632, 1983.

[13] J. Meng, G. Liu, and Z. Li, "A geometric theory for analysis and synthesis of sub-6 DoF parallel manipulators," *IEEE Trans. Robot.*, vol. 23, no. 4, pp. 625–649, Aug. 2007.

[14] Q. Li and J. M. Hervé, "Type synthesis of 3-DOF RPR-equivalent parallel mechanisms," *IEEE Trans. Robot.*, vol. 30, no. 6, pp. 1333–1343, Dec. 2014.

[15] J. F. McGovern and G. N. Sandor, "Kinematic synthesis of adjustable mechanisms—Part 1: Function generation," *J. Eng. Ind.*, vol. 95, no. 2, pp. 417–422, 1973.

[16] R. I. Alizade and Ö Kilit, "Analytical synthesis of function generating spherical four-bar mechanism for the five precision points," *Mech. Mach. Theory*, vol. 40, no. 7, pp. 863–878, 2005.

[17] A. Kunjur and S. Krishnamurty, "Genetic algorithms in mechanism synthesis," *J. Appl. Mech. Robot.*, vol. 4, no. 2, pp. 18–24, 1997.

[18] P. S. Shiakolas, D. Koladiya, and J. Kebrle, "On the optimum synthesis of six-bar linkages using differential evolution and the geometric centroid of precision positions technique," *Mech. Mach. Theory*, vol. 40, no. 3, pp. 319–335, 2005.

[19] J. A. Cabrera, F. Nadal, J. P. Muñoz, and A. Simon, "Multiobjective constrained optimal synthesis of planar mechanisms using a new evolutionary algorithm," *Mech. Mach. Theory*, vol. 42, no. 7, pp. 791–806, 2007.

[20] M. Castelli, L. Vanneschi, and S. Silva, "Semantic search-based genetic programming and the effect of intron deletion," *IEEE Trans. Cybern.*, vol. 44, no. 1, pp. 103–113, Jan. 2014.

[21] P.-H. Kuo, T.-H. S. Li, Y.-F. Ho, and C.-J. Lin, "Development of an automatic emotional music accompaniment system by fuzzy logic and adaptive partition evolutionary genetic algorithm," *IEEE Access*, vol. 3, pp. 815–824, 2015.

[22] B. Yuan, B. Li, H. Chen, and X. Yao, "A new evolutionary algorithm with structure mutation for the maximum balanced biclique problem," *IEEE Trans. Cybern.*, vol. 45, no. 5, pp. 1054–1067, May 2015.

[23] J. H. Holland, *Adaptation in Natural and Artificial Systems*. Ann Arbor, MI, USA: Univ. of Michigan Press, 1975.

[24] C.-H. Chen, T.-K. Liu, and J.-H. Chou, "A novel crowding genetic algorithm and its applications to manufacturing robots," *IEEE Trans. Ind. Informat.*, vol. 10, no. 3, pp. 1705–1716, Aug. 2014.

[25] D. E. Goldberg, *Genetic Algorithms in Search, Optimization & Machine Learning*. Reading, MA, USA: Addison-Wesley, 1989.

[26] J. E. Fieldsend, "Using an adaptive collection of local evolutionary algorithms for multi-modal problems," *Soft Comput.*, vol. 19, no. 6, pp. 1445–1460, 2015.

[27] C.-H. Chen, T.-K. Liu, I.-M. Huang, and J.-H. Chou, "Multiobjective synthesis of six-bar mechanisms under manufacturing and collision-free constraints," *IEEE Comput. Intell. Mag.*, vol. 7, no. 1, pp. 36–48, Feb. 2012.

[28] P. Schneider and D. H. Eberly, *Geometric Tools for Computer Graphics*. San Mateo, CA, USA: Morgan Kaufmann, 2002.

[29] N. Hansen and S. Kern, "Evaluating the CMA evolution strategy on multimodal test functions," in *Parallel Problem Solving From Nature*. Berlin, Germany: Springer, 2004, pp. 282–291.

[30] M. A. Laribi, A. Mlika, A. L. Romdhane, and S. Zeghloul, "A combined genetic algorithm–fuzzy logic method (GA–FL) in mechanisms synthesis," *Mech. Mach. Theory*, vol. 39, no. 7, pp. 717–735, 2004.

[31] K. Nag, T. Pal, and N. R. Pal, "ASMiGA: An archive-based steady-state micro genetic algorithm," *IEEE Trans. Cybern.*, vol. 45, no. 1, pp. 40–52, Jan. 2015.

[32] S. Das, S. Maity, B.-Y. Qu, and P. N. Suganthan, "Real-parameter evolutionary multimodal optimization—A survey of the state-of-the-art," *Swarm Evol. Comput.*, vol. 1, no. 2, pp. 71–88, 2011.

[33] K. A. De Jong, "Analysis of the behavior of a class of genetic adaptive systems," Ph.D. dissertation, Dept. Comput. Commun. Sci., Univ. Michigan, Ann Arbor, MI, USA, 1975.

[34] S. W. Mahfoud, "Niching methods for genetic algorithms," Dept. General Eng., Univ. Illinois Urbana–Champaign, Champaign, IL, USA, Tech. Rep. 95001, 1995.

[35] L. Qing, W. Gang, Y. Zaiyue, and W. Qiuping, "Crowding clustering genetic algorithm for multimodal function optimization," *Appl. Soft Comput.*, vol. 8, no. 1, pp. 88–95, 2008.

[36] K. Deb and R. B. Agrawal, "Simulated binary crossover for continuous search space," *Complex Syst.*, vol. 9, no. 3, pp. 1–15, 1994.

[37] K. Deb, "An efficient constraint handling method for genetic algorithms," *Comput. Methods Appl. Mech. Eng.*, vol. 186, nos. 2–4, pp. 311–338, 2000.

[38] T.-M. Wu and C.-K. Chen, "Mathematical model and its simulation of exactly mechanism synthesis with adjustable link," *Appl. Math. Comput.*, vol. 160, no. 2, pp. 309–316, 2005.

[39] R. L. Norton, *Fundamentals of Machine Design*. Boston, MA, USA: McGraw-Hill, 2004.

CHIU-HUNG CHEN received the B.S. degree in computer engineering from National Chiao Tung University, Shinchu, Taiwan, in 1990, the M.Sc. degree in computer science and information engineering from National Taiwan University, Taipei, Taiwan, in 1992, and the Ph.D. degree in engineering science and technology from the National Kaohsiung First University of Science and Technology, Kaohsiung, Taiwan, in 2009. He is currently an Associate Professor with Kao Yuan University, Kaohsiung. From 1992 to 1999, he was the Manager of the Institute of Information Industry, Taiwan. From 2000 to 2002, he was the Senior Manager of Photon Computer, Taiwan. From 2003 to 2006, he was the Senior Manager of ULead Inc., Taiwan. His research interests include evolutionary computation, multiobjective optimization, intelligent manufacturing, game intelligence, and multimedia system.

JYH-HORNG CHOU (SM'04–F'15) received the B.S. and M.S. degrees in engineering science from National Cheng Kung University, Tainan, Taiwan, in 1981 and 1983, respectively, and the Ph.D. degree in mechatronic engineering from National Sun Yat-sen University, Kaohsiung, Taiwan, in 1988. He is currently a Chair Professor with the Electrical Engineering Department, National Kaohsiung University of Applied Sciences, Taiwan. He has co-authored four books, and published over 275 refereed journal papers. He also holds six patents. His research and teaching interests include intelligent systems and control, computational intelligence and methods, automation technology, robust control, and robust optimization. He was a recipient of the 2011 Distinguished Research Award from the National Science Council of Taiwan, the 2012 IEEE Outstanding Technical Achievement Award from the IEEE Tainan Section, the 2014 Distinguished Research Award from the Ministry of Science and Technology of Taiwan, the Research Award, and the Excellent Research Award from the National Science Council of Taiwan 12 times, and numerous academic awards/honors from various societies. Based on the IEEE Computational Intelligence Society (IEEE CIS) evaluation, his Industrial Application Success Story has got the 2014 winner of highest rank, thus being selected to become the first internationally industrial success story being reported on the IEEE CIS website. He is also a fellow of the Institution of Engineering and Technology, the Chinese Automatic Control Society, the Chinese Institute of Automation Engineer, and the Chinese Society of Mechanical Engineers.